

PACS numbers: 28.60.+s; 52.50.–j; 52.38.–r
DOI: 10.1070/QE2004v034n06ABEH002779

Characteristic time of ion extraction from a plasma bunch in laser isotope separation

V.A. Gundienkov, A.N. Tkachev, S.I. Yakovlenko

***Abstract*. The problem of ion extraction from plane and cylindrical plasma layers located respectively between the plates and coaxial cylinders of a capacitor in laser isotope separation is considered. Simplified analytic models and numerical calculations within the framework of one-dimensional two-fluid hydrodynamics are used. The ion current to the cathode is shown to be adequately described by the three-halves power equation in which the distance of the plasma bunch boundary from the cathode is the electrode separation and the voltage drop across the capacitor plates serves as the voltage difference. The results of calculations are in qualitative agreement with experimental results.**

Keywords: *laser isotope separation, plasma, ion extraction.*

1. Introduction

Ion extraction from a plasma is one of the key processes in the Atomic Vapour Laser Isotope Separation (AVLIS) technique. This process is particularly important in the separation of weight amounts of a rare isotope (see, for instance, reviews [1 – 4]). In this case, there is good reason to distinguish two extraction stages. At the first stage, the ions are drawn out of the plasma bunch and at the second stage they are transported to the collector located in the region of geometrical shadow, where the risk of contamination by the main isotope is small enough. The process of ion extraction from the plasma was simulated in Refs [5 – 9]. The ion transportation through the electrode system was considered in Refs [10, 11].

Note that the selective stepwise ionisation in the laser isotope separation results in the production of a plasma with unique parameters – a low temperature and a high degree of ionisation, which are hard to achieve by other techniques. These peculiar properties were discussed in Refs [6 – 9].

For a high yield of a rare isotope, the restrictions of extraction currents caused by the space charge of a plasma column and the resulting increase in the characteristic time of extraction of the bulk of ions from the plasma become significant. For the collection of the resultant ions to be efficient, this time should be shorter than the time between of the laser pulses for the vapour ionisation. Our work is concerned with consideration of characteristic ion extraction times.

In the general case, the problem of ion extraction from a plasma should be considered using the two-dimensional or even three-dimensional geometry, which is rather complicated to realise. However, the main features of the physics of the process can be elucidated in the context of one-dimensional problems – plane or cylindrical. Furthermore, this approach is of interest, because it permits obtaining some analytic results and compare them with the numerical solution and experiments [12].

2. Estimate of the ion extraction time from the three-halves power law

Planar geometry. Consider a planar plasma layer in a plane capacitor (Fig. 1a) with a voltage drop U across its plates. Owing to a fast charge transfer by the electron current, the plasma potential sets in to become approximately equal to the cathode potential. The subsequent ion extraction proceeds during a time shorter than the electron times, so that the ion current is compensated for by the electron current to the anode and the plasma potential is maintained close to the anode potential. We will describe the extraction process using the well-known Child – Langmuir three-halves power law [13 – 15] for the ion current density from a unit surface area of the plasma layer

$$j_\mathrm{i} = a_\mathrm{pl}\frac{U^{3/2}}{(x_\mathrm{c}-x)^2},\quad a_\mathrm{pl} \equiv \frac{1}{9\pi}\left(\frac{2e}{m_\mathrm{i}}\right)^{1/2} \approx 4.3\times 10^{-9}\ \mathrm{V}^{-3/2}\mathrm{A}. \quad (1)$$

Here, x_c is the initial distance between the middle of the plasma layer and the cathode; x is the variable coordinate of the plasma layer boundary nearest to the cathode; and m_i is the ion mass. The mass of a gadolinium ion is taken for a specific estimate: $m_\mathrm{i} = Am_\mathrm{p}$, $A = 157$, and m_p is the proton mass.

We will determine the ion extraction time assuming that an ion charge leaves the immobile plasma boundary nearest to the cathode and in this case the plasma boundary – cathode distance $x_\mathrm{c} - x$ changes, so that according to the ion number conservation law $eN_\mathrm{i}\mathrm{d}x = -j_\mathrm{i}(x)\mathrm{d}t$ (e is the electron charge and N_i is the ion density in the plasma layer). We employ expression (1) to obtain the equation for the plasma boundary coordinate $x(t)$:

V.A. Gundienkov, A.N. Tkachev, S.I. Yakovlenko A.M. Prokhorov General Physics Institute, Russian Academy of Sciences, ul. Vavilova 38, 119991 Moscow, Russia

Received 23 December 2003
Kvantovaya Elektronika **34** (6) 589 – 595 (2004)
Translated by E.N. Ragozin

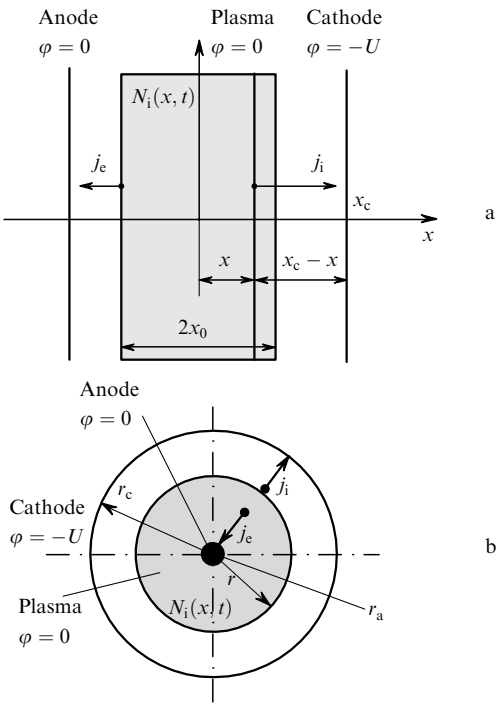

Figure 1. Plasma layer in plane (a) and cylindrical (b) capacitors: x is the distance between the middle of the plasma layer and the variable boundary of the region occupied by the plasma; φ is the potential at different points (the potential in the plasma and at the left capacitor plate is assumed to be the same); $2x_0$ is the initial width of the plasma layer; and $x_c - x_0$ is the initial distance between the plasma layer boundary and the capacitor plate.

$$\frac{dx}{dt} = -\frac{j_i(x)}{eN_i} = -\frac{a_{pl}U^{3/2}/eN_i}{(x_c - x)^2},$$

By integrating this equation, we obtain the following expressions for the time dependences of the cathode–plasma boundary distance $y(t) = x_c - x(t)$ and of the current density on the collector $j_i(t)$, and also for the total time taken to extract all ions from the layer:

$$y(t) = x_c[3t/\tau_c + (y_0/x_c)^3]^{1/3}, \tag{2a}$$

$$j_i(t) = \frac{j_0}{[3t/\tau_c + (y_0/x_c)^3]^{2/3}} \text{ for } 0 < t < \tau_0, \tag{2b}$$

$$\tau_0 = 2\left[\frac{x_0}{x_c} + \frac{(x_0/x_c)^3}{3}\right]\tau_c. \tag{2c}$$

Here, x_0 is the initial half-width of the plasma layer; $j_0 = a_{pl}U^{3/2}/x_c^2$ is the current density for $x(t) = 0$;

$$\tau_c = \frac{ex_c^3N_i}{a_{pl}U^{3/2}} = \frac{9\pi}{\sqrt{2}}(m_ie)^{1/2}\frac{x_c^3N_i}{U^{3/2}}$$

$$= 3.69\times10^{-11}\frac{x_c^3N_i}{U^{3/2}} \tag{3}$$

is the characteristic decay time of the current density on the collector (in seconds); and $x(t_0) = -x_0$; U is measured in volts. Note that the current density is infinite for $x_0 = x_c$ at the initial instant of time $t = 0$. For $U \approx 500$ V, $N_i \approx 10^{10}$ cm^{-3}, $x_0 = 0.5$ cm, and $x_c = 1$ cm, we have $\tau_c = 33$ μs and $\tau_0 = 35.6$ μs.

Cylindrical geometry. The problem of the limiting current has no analytic solution in the case of cylindrical geometry (see Fig. 1b). The three-halves power law remains valid, but a simple dependence of the current on the electrode separation is absent. This problem was first solved by Langmuir and Blodgett and by Boguslavskii (for more details, see Refs [13–15]). They represented the ion current per unit length of the cylinder in the form:

$$i_i = a_{cyl}\frac{U^{3/2}}{r_a\beta^2(r_c/r_a)},$$
$$a_{cyl} \equiv \frac{2}{9}\left(\frac{2e}{m_i}\right)^{1/2} = 2\pi a_{pl} \approx 2.7\times10^{-8}\ \text{V}^{-3/2}\,\text{A}. \tag{4}$$

Here, r_c and r_a are the radii of the cathode and anode, respectively; $\beta^2(x)$ is defined in the form of a power-fractional series in $z = \ln x$; $x = r/r_a$; and r is the distance to the axis of the cylinders.

At the present time it is simpler to solve numerically the initial equation than perform the series summation. Indeed, proceeding from the Poisson equation for the potential φ, the definition of current i in terms of charged particle velocities v_i, and the energy conservation law,

$$\frac{1}{r}\frac{d}{dr}\left(r\frac{d\varphi}{dr}\right) = 4\pi eN_i, \quad i = 2\pi reN_iv_i, \quad m_iv_i^2/2 = e\varphi,$$

we arrive at the Child equation:

$$\frac{d^2u}{dz^2} = \frac{\exp z}{\sqrt{u}}, \quad u(z)|_{z\to1} = \left.\frac{du}{dz}\right|_{z\to1} = 0. \tag{5}$$

Here, $u = \varphi(a_{cyl}/ir_c)^{3/2}$ is the dimensionless potential. In this case, we have $\beta^2(x_d) = u^{3/2}/x_d$ (where x_d is the cathode–anode distance). The dependence $\beta^2(r_c/r_a)$ constructed on the basis of numerical solution of (5) is plotted in Fig. 2.

The ion extraction time will be determined under the same assumptions as in the planar case, proceeding from the charge conservation law:

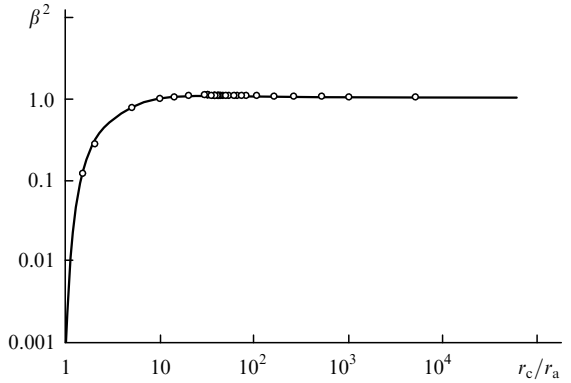

Figure 2. Dependence of the correction factor β^2 in the three-halves power law on r_c/r_a. The solid curve was obtained by solving numerically the Child equation (5); the circles represent the calculation carried out on the basis of the Boguslavskii series [13].

$$\frac{\mathrm{d}}{\mathrm{d}t}(\pi r^2 N_\mathrm{i}) = -i_\mathrm{i}, \quad \frac{\mathrm{d}r}{\mathrm{d}t} = -\frac{i_\mathrm{i}}{2\pi r N_\mathrm{i}}.$$

We employ the three-halves power law (4) for the current to obtain

$$\frac{\mathrm{d}r}{\mathrm{d}t} = -\frac{1}{\beta^2(r_\mathrm{c}/r)(r_\mathrm{c}/r)} \frac{U^{3/2}}{9\pi r_\mathrm{c}^2 N_\mathrm{i}} \left(\frac{2}{m_\mathrm{i} e}\right)^{1/2}, \quad r(t)|_{t=0} = r_0.$$

By solving this equation, we obtain

$$t/\tau_\mathrm{c} = \int_{r_\mathrm{c}/r_0}^{r_\mathrm{c}/r} \beta^2(x) x^{-3} \mathrm{d}x,$$
$$\tau_\mathrm{c} = \frac{9\pi}{\sqrt{2}} (m_\mathrm{i} e)^{1/2} \frac{r_\mathrm{c}^3 N_\mathrm{i}}{U^{3/2}} = 3.7 \times 10^{-11} \frac{r_\mathrm{c}^3 N_\mathrm{i}}{U^{3/2}}. \tag{6}$$

The quantity $x_\mathrm{c} \leftrightarrow r_\mathrm{c}$ is defined, correct to the change τ_c, by expression (3), and U is measured in volts.

If, at the initial instant of time $t = 0$, the plasma touches the cathode ($r_0 = r_\mathrm{c}$) and the anode radius is much smaller than the cathode radius ($r \ll r_\mathrm{c}$), the departure time for all ions is determined by the expression

$$\tau_\mathrm{max} = \tau_\mathrm{c} \int_1^\infty \beta^2(x) x^{-3} \mathrm{d}x \approx 0.095 \tau_\mathrm{c}. \tag{7}$$

For instance, for $U > 500$ V, $N_\mathrm{i} \approx 10^{10}$ cm^{-3}, and $r_\mathrm{c} = 1$ cm, we have $\tau_\mathrm{c} = 33$ μs and $\tau_0 = 3.1$ μs. For the same parameters and $r_\mathrm{c} = 10$ cm, the times are one thousand times longer: $\tau_\mathrm{c} = 33$ ms and $\tau_0 = 3.1$ ms.

The models considered above are valid when the plasma boundary motion due to gas-dynamic expansion can be neglected, so that the ion extraction from the plasma proceeds faster than its expansion. In fact, as a rule, the characteristic times of plasma bunch expansion and ion extraction are of the same order of magnitude. This is due to the fact that the ionisation-pulse repetition rate should approximately correspond to the time of vapour replacement in the ionisation region. The characteristic plasma expansion time is, as a rule, approximately equal to the time of vapour flight through the ionisation region. Since the plasma boundary approach to the cathode owing to the expansion improves the extraction conditions rather than impairing them, the above model would be expected to yield somewhat overestimated ion extraction times compared to the experimental ones.

3. Calculations within the framework of a one-dimensional transient model

3.1 Planar geometry

On the planar model. Consider the mechanism of ion extraction in the regime when the plasma expansion is significant using a one-dimensional transient two-fluid hydrodynamic model. The mathematical formulation of the problem and the solution algorithm for the equations of this model are described in Refs [6–9]. Here, we give only some of the data required for the understanding of the results of calculations presented below.

The plasma is characterised by the electron and ion densities N_e and N_i, which depend on the time t and the distance x to the centre of the planar layer, by the hydrodynamic velocities v_e and v_i, and also by the electron pressure p_e. These quantities are obtained by solving numerically the equations of two-fluid hydrodynamics in the Lagrangian coordinate system. The ion temperature is assumed equal to zero. The electron pressure and the electron temperature T_e are related by the adiabatic Poisson law $T_\mathrm{e} \propto N_\mathrm{e}^{\gamma-1}(\gamma = 3)$. The electric field is characterised by the intensity $E = -\partial\varphi/\partial x$ and the potential φ. These quantities are obtained by solving the Poisson equation.

The two-fluid hydrodynamic problem was treated in dimensionless quantities. The lengths were measured in Debye radii: $l_0 = r_\mathrm{D} = [T_\mathrm{e0}/(4\pi e^2 N_0)]^{1/2}$; the time in the reciprocals of the Langmuir frequencies: $t_0 = \omega_\mathrm{L}^{-1} = [m_\mathrm{e}/(4\pi e^2 N_0)]^{1/2}$; the velocities in units of the characteristic initial thermal electron velocities: $v_0 = (T_\mathrm{e0}/m_\mathrm{e})^{1/2}$; the potential φ_0 and the electric intensity E_0 were expressed in terms of the initial electron temperature: $\varphi_0 = T_\mathrm{e0}/e$, $E_0 = T_\mathrm{e0}/el_0$. The density and pressure were normalised to the maximum values of the initial electron density (N_0) and pressure (p_e0), in this case $n_\mathrm{e} = N_\mathrm{e}/N_0$ and $T_0 = p_\mathrm{e0}/N_0$.

In the calculations given here, the initial density distribution was assumed to be uniform on the segment $x \in [-x_0, x_0]$. The plasma was assumed to be immobile and quasi-neutral at the initial instant of time.

We used in our calculations an artificially overstated electron-to-ion mass ratio $\mu = m_\mathrm{e}/m_\mathrm{i} = 10^{-2}$. The dependence of the steady-state average electron and ion velocities and of the characteristic settling time for the electron and ion fluxes on μ was investigated in Refs [6–9]. Calculations suggest that the velocities are proportional to $1/\sqrt{\mu}$ and the characteristic mass-average velocity settling time $\propto\sqrt{\mu}$ (for more details, see Ref. [8]). We employed these dependences to scale the data obtained by numerical calculations to the value of $\mu \approx 3.5 \times 10^{-6}$ (for the gadolinium plasma).

Results of calculation of the time evolution of the plasma layer. The results of one of the variants of calculation of the time evolution of the plasma layer are presented in Figs 3–5. We used the following values of parameters: $N_\mathrm{e} = 10^{10}$ cm^{-3}, $T_\mathrm{e} = 0.015$ eV, $x_0 = 0.5$ cm, $x_\mathrm{c} = 1$ cm, $U = 400$ V, and $A = 157$ (gadolinium).

For the parameters involved, the field induced by capacitor plates is weak in the sense that it is not able to completely separate the charges of the plasma layer: $E \ll 8\pi e x_0 N_\mathrm{e} \approx 2 \times 10^4$ V cm^{-1}. For this reason the ion extraction process has the quasi-stationary nature described below.

The electric field inside the plasma layer is almost completely screened, in this case the electron and ion densities being almost the same (see Fig. 3). Outside the plasma layer, ions prevail on the cathode side and electrons prevail on the anode side. The densities of extracted electrons and ions are low compared to the plasma density, and this determines the quasistationary nature of the electron and ion extraction process. Because of a small mass, a part of the electrons flows from the plasma layer to the anode at the initial instant of time. As a result, the plasma layer acquires a potential close to the anode potential. Accordingly, the electric field in the plasma layer–anode gap becomes small compared to the field in the layer–cathode gap (Figs 3b–3d). Subsequently, the electron current to the anode maintains the layer potential close to the anode potential, and therefore its magnitude is determined by the ion current to the cathode.

In the cathode–plasma layer gap there occurs field screening by the ions being extracted. The dependence of

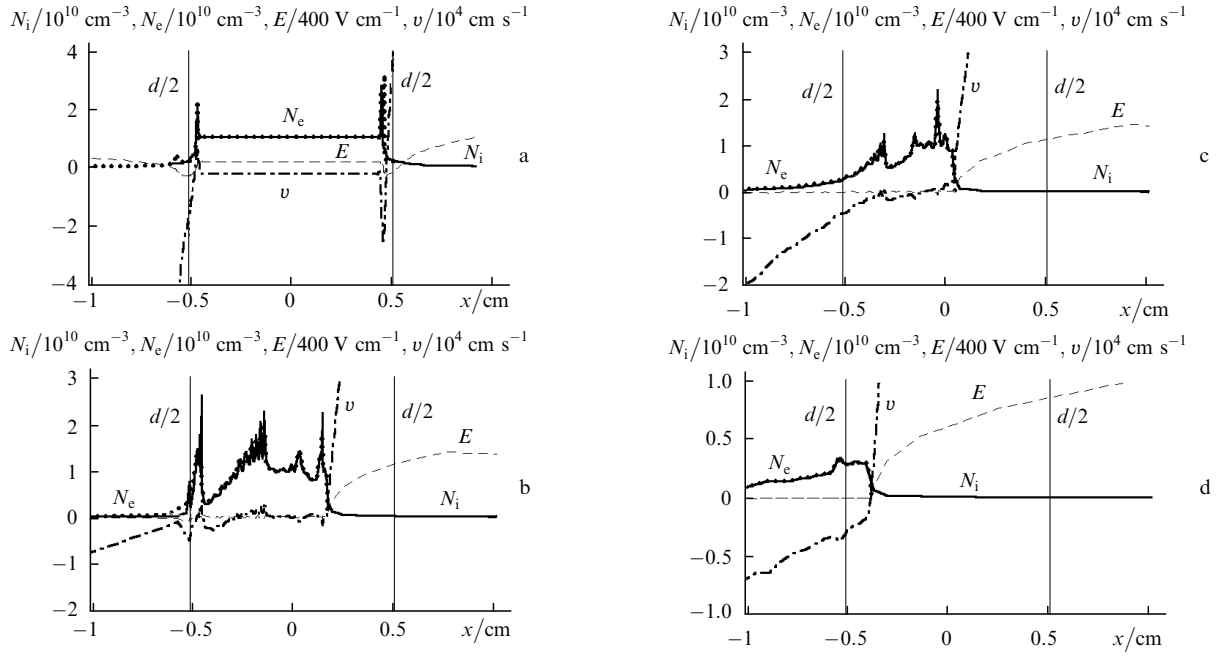

Figure 3. Distributions (planar geometry) of the ion (N_i) and electron (N_e) densities as well as of the field intensity E and ion velocity v over the coordinate x at the instants of time $t\omega_L = 24$ (a), 172 (b), 264 (c), and 1007 (d). The potential difference between the capacitor plates is $U = 400$ V; the mass ratio is $\mu = 10^{-2}$. Here and in Fig. 4 the thin vertical lines indicate the initial position of the plasma boundaries.

the electric field on the coordinate x in the gap between the plasma boundary (with a coordinate x_b) and the cathode is well described by the expression $E(x) \propto (x - x_b)^{1/3}$, which follows from the Child equation underlying the three-halves power law.

It is interesting that the plasma layer as if moves to the anode as a whole, which is evident from Fig. 3 and particularly from the $x - t$ diagram (Fig. 4), which demonstrates the time evolution of plasma layer boundaries. The motion of the plasma bunch boundary adjacent to the cathode is determined by the electron density boundary, which shifts during the ion extraction. It moves somewhat slower than is predicted by expression (2a) because this expression neglects the hydrodynamic expansion of the layer. Note that the slowing down of the boundary motion should result in a shortening of the time of ion extraction from the layer compared to the time which follows from expression (2b) (when the boundary motion slows down, the current from the layer to the cathode is higher than the current used in the estimate). The motion of the plasma bunch boundary adjacent to the anode is determined by the expansion of the ion component. This boundary propagates at a velocity $u_b = 3.3 \times 10^5$ cm s^{-1}, which is 25 times higher than the thermal velocity $v_T = (2T_e/m_i)^{1/2} = 1.4 \times 10^4$ cm s^{-1}. So high a boundary propagation velocity is caused by the Coulomb explosion of the uncompensated ion charge in the thin surface layer of the bunch [5, 8]. The bulk

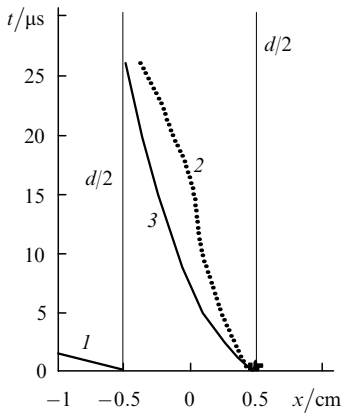

Figure 4. The $x - t$ diagram characterising the motion of plasma boundaries (planar geometry): (*1*) ion density boundary adjacent to the anode; (*2*) electron density boundary adjacent to the cathode; (*3*) calculation by formula (2a).

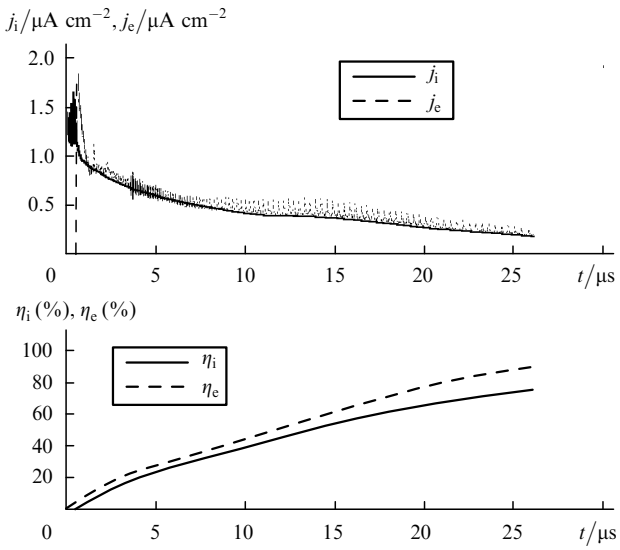

Figure 5. Time dependences of the ion (j_i) and electron (j_e) current densities (a) as well as fractions of the total electron (η_e) and ion (η_i) layer charges picked up at the collectors (b) (planar geometry).

of the ions expand towards the anode at a velocity of the order of the thermal velocity (see Figs 3b–3d).

The ion current to the cathode corresponds closely to the three-halves power law in which the position of the plasma boundary $x(t)$ nearest to the cathode is taken from the numerical calculation (see Fig. 4). Note also that the gas-dynamic layer expansion results in a lowering of the fraction of ions collected at the cathode as compared to the immobile plasma case (for the initial temperature). It is likely that the fraction of ions collected at the cathode would become lower with increasing the initial electron plasma temperature and also with decreasing the anode–layer distance.

3.2 Cylindrical geometry

On the cylindrical model. To elucidate the effect of geometry on the ion extraction mechanism, we considered a cylindrical expansion model of the plasma located between coaxial cylinders (see Fig. 1b). In all other respects, the mathematical model corresponded to the case of planar geometry described above, i.e., we considered a two-fluid transient hydrodynamics and employed the same procedure involving dimensional extraction times and their scaling to the physical electron-to-ion mass ratio.

By and large the scheme of calculations remained unchanged. Only the scheme of calculating the electric field was refined: a bilinear interpolation was used instead of the linear one.

Note the specific character of calculations in cylindrical geometry related to the use of scaling with respect to the mass ratio. In the cylindrical case, assuming a relatively short anode radius and a moderate value of μ, a situation may be realised whereby the current is limited not by the space charge of the ions in the plasma–cathode gap but by the space charge of the electrons in the plasma–anode gap. In this case, even though the quasistationary sink pattern may persist, the scaling of computed quantities to the physical values of mass ratios on the basis of scale ratios may lead to incorrect results. To avoid this, the anode radius should be taken large enough, so that the electron current (obtained by an estimate by the three-halves power law) in the anode–plasma gap for a given mass ratio should be several times higher than the ion current in the plasma–cathode gap.

Results of calculations. The results of calculations of one of the variants of the time evolution of the plasma layer are presented in Figs 6–8. We assume in calculations that the initial ion and electron densities were identical ($N_e = N_i = 10^{10}$см$^{-3}$) on the segment $r \in [r_{01}, r_{02}] = [0.075$ cm, 0.575 cm]; the plasma was assumed to be initially immobile, and the remaining parameters of the problem were as follows: $T_e = 0.0145$ eV, $U = 400$ V, and $A = 157$ (gadolinium).

By and large the pattern of charge sink from the plasma in the cylindrical case repeats the sink pattern in the planar case. As in the planar case, the field in the cathode–plasma layer gap is screened by the ions being extracted. The dependence of the electric field in the plasma boundary–cathode gap on the coordinate, as in the planar case, is well described by the Child equation.

As expected, the velocity of plasma boundary motion in the cylindrical case (see the $r-t$ diagram in Fig. 7) is somewhat lower than in the planar case. The reduction of

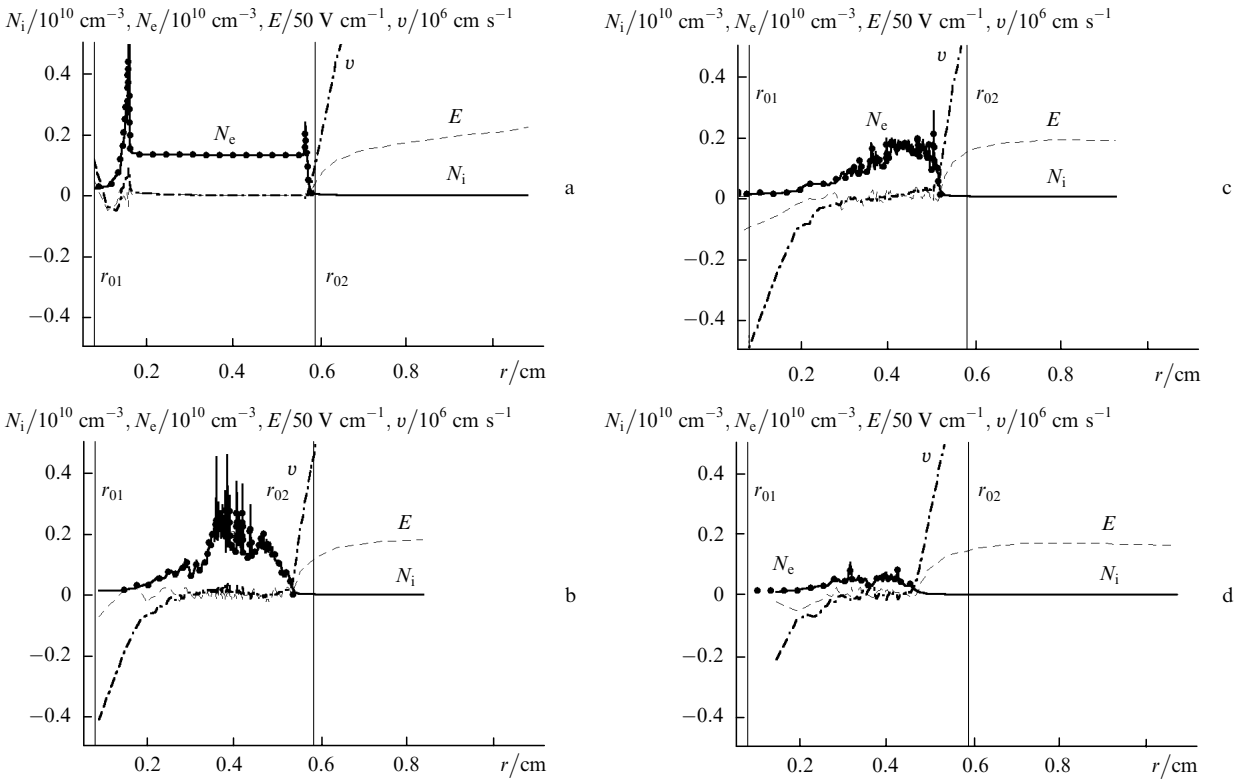

Figure 6. Distributions (cylindrical geometry) of the ion (N_i) and electron (N_e) densities as well as of the field intensity E and ion velocity v over the coordinate r at instants of time $t\omega_L = 38$ (a), 445 (b), 727 (c), and 1480 (d). The potential difference between the capacitor plates is $U = 400$ V; the mass ratio is $\mu = 10^{-2}$; r_{01} and r_{02} are the respective radii of the inner and outer boundaries of the plasma layer. The distributions are given in the interval between the anode and the cathode $r_a \leqslant r \leqslant r_c$.

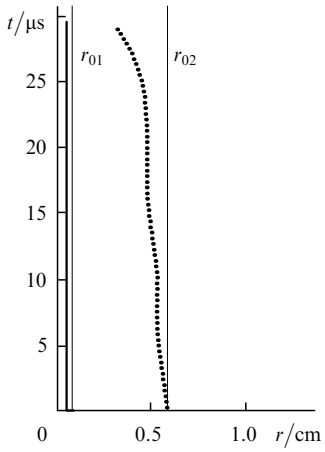

Figure 7. The $r-t$ diagram characterising the motion of plasma boundaries (cylindrical geometry); the bold solid line is the ion density boundary adjacent to the anode, the dotted line is the electron density boundary adjacent to the cathode.

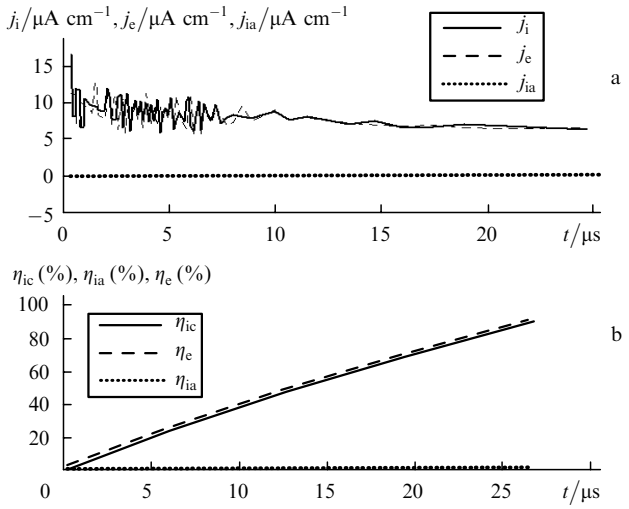

Figure 8. Time dependences of the ion (j_i), electron (j_e), and anode ion (j_{ia}) current densities (a) as well as of the fractions of the total electron charge (η_e) and of the ion charges at the cathode (η_{ic}) and the anode (η_{ia}) picked up at the collectors (b) (cylindrical geometry).

the velocity of motion is related to the fact that the major part of plasma column charge for small anode radii is concentrated in the peripheral layers of the bunch.

Upon ion extraction in cylindrical geometry, the anode–plasma gap is usually minimised (for instance, by placing a wire at the centre of the plasma bunch as the anode). A peculiarity of the extraction in this geometry is that the plasma flow to the anode is significantly higher than in the planar geometry (in the case under consideration, the counterpressure of the peripheral plasma layers which limits the velocity of thermal expansion in the planar case vanishes almost at once, see Fig. 8). Because of the thermal expansion of the column, up to 20 % – 30 % of the plasma ions arrived at the anode in the calculations described.

4. Comparison with experimental results

The results of measurements of the time of ion extraction from a cylindrical bunch of laser-produced gadolinium plasma in a plane capacitor were reported in Ref. [12]. The ion extraction was investigated in two configurations. In one configuration, the plasma cylinder was located between the capacitor plates across which a voltage U was applied. In the other case, the capacitor plates were at the same potential, but a wire charged at a voltage U relative to the capacitor plates was introduced into the plasma. The initial diameter of the plasma cylinder was ~ 1 cm, the initial distance between the plasma boundary and the capacitor plate was 0.5 cm (the capacitor plate separation was 2 cm). The initial ion and electron densities in the plasma were varied in the range $N_{e0} = N_{i0} \approx (0.1 - 4) \times 10^{10}$ cm^{-3}.

Simulation of the experimental conditions of Ref. [12] calls for the consideration of a two-dimensional problem. However, we compared the calculations and estimates made within the framework of a one-dimensional model with experimental results in the hope of attaining agreement by an order of magnitude. The experimental dependence of ion extraction time on the voltage across the plasma–ion collector gap is in qualitative agreement with the results of calculations both in planar and cylindrical geometry (Fig. 9). The results of calculations in cylindrical geometry are in better agreement with the experiments on ion extraction from the column with a wire introduced inside of it and the results of calculations in the planar geometry with the experiments on ion extraction from the column located between the capacitor plates. The experimental and calculated data diverge by no more than a factor of two. The estimates of extraction times by formula (2b) turned out to

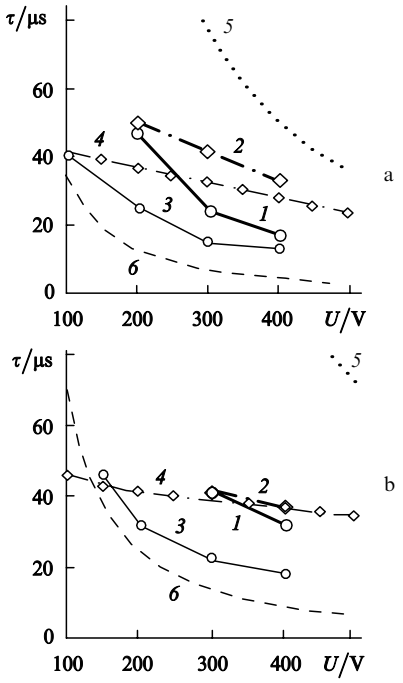

Figure 9. Dependences of the time of ion extraction from the plasma on the voltage U for $N_{e0} = N_{i0} = 10^{10}$ cm^{-3} (a) and $N_{e0} = N_{i0} = 2 \times 10^{10}$ cm^{-3} (b): (*1*, *2*) planar geometry with calculations corresponding to the experimental conditions when the plasma cylinder is located between the capacitor plates at a voltage U; (*3*, *4*) cylindrical geometry with a potential difference applied across the wire inside the plasma and the capacitor plates [(*3*) experiment of Ref. [11], (*4*) calculation of plasma layer expansion in the capacitor]; (*5*) calculation by formulas (2c) and (3) for a plane layer of thickness $2x_0 = 1$ cm; (*6*) calculation by formula (7) for a cylindrical layer and $r = 0.5$ cm.

be, as would be expected, 2–4 times higher than the experimental values.

For the experiments with a wire embedded in the plasma, the effective thickness of the plasma layer is approximately two times smaller than in the case when the ion extraction proceeds due to the voltage across the capacitor plates. According to formula (2b), the ion extraction time in the experiments with a wire should be significantly (3.7 times) shorter than in the experiments involving ion collection to the capacitor plates. This statement is qualitatively consistent with experimental results; however, the reduction of ion extraction time was less significant (by a factor of 1.5–2).

5. Conclusions

The following conclusions can be drawn from the above consideration of the mechanism of ion extraction in laser isotope separation.

When the plasma is embedded in a relatively weak electric field which cannot pull out all electrons and ions from the plasma bunch, the ion extraction process is quasi-stationary. Some electrons escape from the plasma bunch, which acquires a potential close to the anode potential. The ion current to the cathode is adequately described by the three-halves power law in which the distance of the plasma bunch boundary from the cathode serves as the electrode separation and the voltage drop across the capacitor plates serves as the voltage difference. Therefore, the ion extraction time is determined by the integration of the ion current determined by the three-halves power equation. The corresponding estimates and calculations are in qualitative agreement with the available experimental data.

References

1. Yakovlenko S.I. *Kvantovaya Elektron.*, **25** (11), 971 (1998) [*Quantum Electron.*, **28** (11), 945 (1998)].
2. *Laser and Particle Beams*, **16** (4), 541 (1998).
3. Yakovlenko S.I. *Adv. in Laser and Opt. Res.*, **1**, 53 (2002).
4. Tkachev A.N., Yakovlenko S.I. *Kvantovaya Elektron.*, **33** (7), 581 (2003) [*Quantum Electron.*, **33** (7), 581 (2003)].
5. Tkachev A.N., Yakovlenko S.I. *Kvantovaya Elektron.*, **20** (11), 1117 (1993) [*Quantum Electron.*, **23** (11), 972 (1993)].
6. Savel'ev V.V., Yakovlenko S.I. *Kvantovaya Elektron.*, **23** (11), 1020 (1996) [*Quantum Electron.*, **26** (11), 994 (1996)].
7. Savel'ev V.V., Yakovlenko S.I. *Kratk. Soobshch. Fiz.*, (11-12), 57 (1996).
8. Savel'ev V.V., Yakovlenko S.I. *Laser Phys.*, **7** (2), 437 (1997).
9. Savel'ev V.V., Yakovlenko S.I. *Kvantovaya Elektron.*, **24** (10), 939 (1997) [*Quantum Electron.*, **27** (10), 913 (1997)].
10. Golyatina R.I., Syts'ko Yu.I., Yakovlenko S.I. *Laser Phys.*, **8** (4), 860 (1998).
11. Golyatina R.I., Syts'ko Yu.I., Yakovlenko S.I. *Kratk. Soobshch. Fiz.*, (7), 3 (1996).
12. Ogura K., Arisawa T., Shibata T. *Jap. J. Appl. Phys.*, (5a), 1485 (1992).
13. Kaptsov N.A. *Elektronika* (Electronics) (Moscow: GITTL, 1954).
14. Granovskii V.L. *Elektricheskii tok v gaze. Ustanovivshiisya tok* (Electric Current in Gases. Steady-State Current) (Moscow: Nauka, 1971).
15. Forrester A.T. *Large Ion Beams: Fundamentals of Generation and Propagation* (New York: Wiley, 1988; Moscow: Mir, 1991).